Supporting Information for

"Protonic Gating of Excited-State Twisting and Charge Localization in GFP Chromophores: A Mechanistic Hypothesis for Reversible Photoswitching"

Seth Olsen, Krissie Lamothe and Todd J. Martínez

I. Schematic Depiction of Hypothetical Photoswitching Mechanism

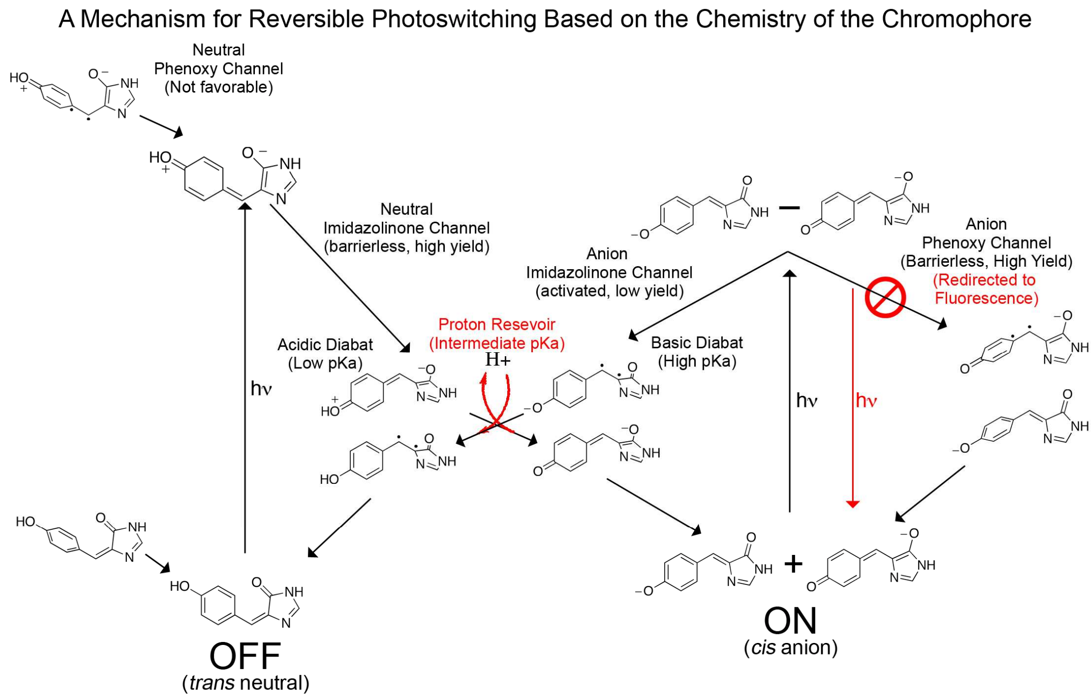

Here, we show a schematic outline of a proposed mechanistic hypothesis for RSFP photoswitching based on the chemistry of the HBI chromophore. Roles for which we invoke the protein are highlighted in red. The reader may verify that the Lewis structures drawn here are consistent with the S_1-S_0 difference density isosurfaces shown in Fig. 2 of the main text. Energies are not drawn to scale.

II: AIMS Simulations

AIMS simulations were carried out using an implementation[1] within the Molpro[2] software. The electronic structure model was generated using a 2-electron, 2-orbital, 2-state-averaged[3] complete active space self consistent field[4] ansatz with a 6-31G Gaussian basis set[5-7] (SA2-CAS(2,2)/6-31G). The timestep was 20a.u. Initial conditions were sampled from a Wigner distribution generated with the S_0 minimum and normal modes calculated using MP2[8]/6-31G**.[5-7] Trajectories were propagated for 20000 a.u. Tables S1.1 and S1.4 describe geometries used to generate the Wigner distribution for anionic and neutral HBI, respectively. Tables S1.2-S1.3 and S1.5-S1.6 list the SA2-CAS(2,2)/6-31G state-specific energies, harmonic frequencies, and natural orbitals and occupation numbers at these geometries.

The MR-RSPT2[9] excitation energy at the SA2-CAS(2,2)/6-31G S_0 minimum of anionic HBI is 2.55eV (468nm). This is quite close to the absorption energy of wild-type GFP (2.61eV; 475nm)[10] and the gas-phase absorption maximum of a GFP chromophore model in its anionic state (2.59eV; 479nm).[11] The MR-RSPT2 excitation of neutral HBI is 3.38eV (367nm), which is in slightly worse agreement with the relevant protein absorption (3.14eV; 397nm)[10] and (corrected) gas phase absorption maxima (3.11eV; 399nm).[12]

Table S1.1. Cartesian coordinates (a.u.) for anionic HBI used to generate the initial distribution for AIMS simulations. Geometry was generated via optimization with MP2/6-31G**.

N	0.00023	0.02264	0.00827
N	0.00239	0.77965	-2.10943
H	-0.00099	0.02721	1.01390
H	-0.00191	2.12329	-0.46607
H	0.00849	-2.50685	-2.96481
H	0.00573	0.98916	-4.48510
H	0.00891	1.35096	-6.93670
H	0.01607	-2.91424	-7.57727
H	0.01289	-3.27044	-5.13169
C	0.00008	1.10898	-0.83967
C	0.00445	-0.62319	-2.12224
C	0.00309	-1.15891	-0.76587
C	0.00739	-1.45104	-3.23701
C	0.00914	-1.17016	-4.61287
C	0.00800	0.14941	-5.16885
C	0.00984	0.34719	-6.52491
C	0.01294	-0.74482	-7.48993
C	0.01391	-2.07163	-6.89442
C	0.01205	-2.26089	-5.53691
O	0.00411	-2.31093	-0.30035
O	0.01420	-0.55340	-8.73406

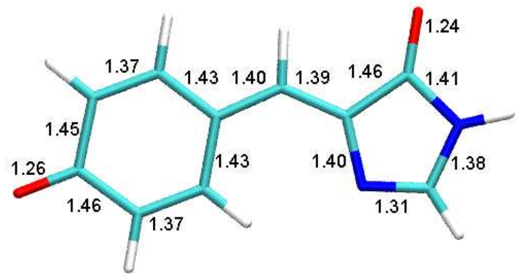

Table S1.2. SA2-CAS(2,2)/6-31G wavefunction (natural orbitals and occupation numbers) at the geometry of anionic HBI detailed in Table S1.1. State Energies: $E(S_0)$= -641.129989161311 a.u., $E(S_1)$= -640.979139746473 a.u.

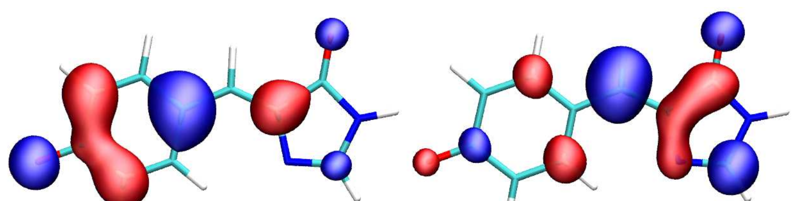

Table S1.3. MP2/6-31G** harmonic frequencies (cm^{-1}) used to generate the ground state Wigner distribution for HBI anion.

52.4121000000	61.6593000000	101.7936000000	116.7688000000
183.2224000000	213.5570000000	240.2600000000	284.7446000000
334.4425000000	368.3210000000	400.1006000000	450.2914000000
463.9662000000	480.9397000000	555.1830000000	591.6552000000
622.0361000000	647.0939000000	692.9289000000	700.9552000000
749.5135000000	775.1792000000	802.6306000000	810.9847000000
838.6382000000	868.9889000000	882.8089000000	914.0303000000
914.9919000000	924.6879000000	997.1300000000	1080.9844000000
1102.6779000000	1123.6264000000	1200.6318000000	1226.4316000000
1296.1302000000	1322.9570000000	1330.1992000000	1389.4409000000
1417.2462000000	1420.1290000000	1485.3904000000	1530.7001000000
1563.4814000000	1596.3911000000	1645.7286000000	1695.7173000000
1727.3166000000	1782.0950000000	3181.3867000000	3197.5202000000
3235.9754000000	3245.1497000000	3269.4591000000	3285.0180000000
3746.4533000000			

Table S1.4. Cartesian coordinates (a.u.) for neutral HBI used to generate the initial distribution for AIMS simulations ('Geometry.dat' file). Geometry was generated via optimization with MP2/6-31G**. Structure is shown at right with bond lengths in Å.

N	-0.01502	0.00026	-0.05085
H	-0.01976	0.00074	0.95599
C	1.08756	-0.00011	-0.87987
H	2.08898	0.00013	-0.47340
N	0.81731	-0.00077	-2.15707
C	-0.58881	-0.00091	-2.22018
C	-1.16969	-0.00017	-0.84788
O	-2.33157	-0.00009	-0.45898
C	-1.37597	-0.00157	-3.32725
H	-2.44144	-0.00152	-3.10878
C	-1.00098	-0.00231	-4.72707
C	0.33519	-0.00245	-5.17491
H	1.13600	-0.00199	-4.44924
C	0.61915	-0.00318	-6.53528
H	1.65093	-0.00328	-6.87088
C	-0.41798	-0.00378	-7.47563
C	-1.74917	-0.00365	-7.04927
H	-2.53641	-0.00411	-7.79111
C	-2.03028	-0.00292	-5.68993
H	-3.06283	-0.00282	-5.35989
O	-0.19636	-0.00450	-8.82712
H	0.75694	-0.00451	-8.98240

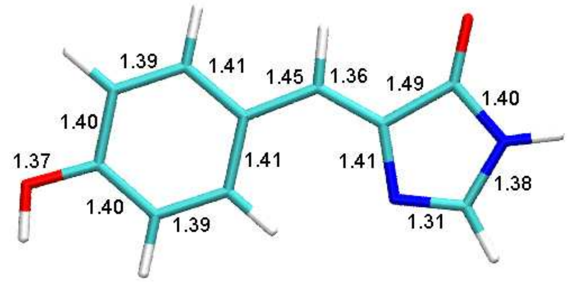

Table S1.5. SA2-CAS(2,2)/6-31G wavefunction (natural orbitals and occupation numbers) at the geometry of neutral HBI detailed in Table S1.4. State Energies: E(S_0)= -641.684182702957 a.u., E(S_1)= -641.500871462917 a.u.

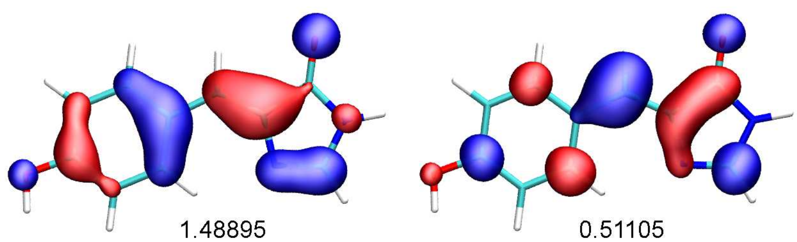

Table S1.6. MP2/6-31G** harmonic frequencies (cm^{-1}) used to generate the ground state Wigner distribution for HBI neutral.

37.9758000000	58.7536000000	105.5490000000	124.4259000000
196.8427000000	213.8970000000	278.6459000000	285.4077000000
345.8032000000	359.8814000000	389.1073000000	407.5105000000
416.8618000000	485.2122000000	496.4213000000	508.9146000000
596.5547000000	634.1109000000	642.9239000000	687.2128000000
730.3536000000	780.7820000000	801.7022000000	807.4762000000
857.1062000000	871.2237000000	878.6276000000	882.5684000000
894.0829000000	905.0130000000	908.7633000000	1041.0747000000
1071.4765000000	1117.5213000000	1147.6811000000	1216.0840000000
1222.8420000000	1235.0734000000	1297.5624000000	1330.7921000000
1345.7579000000	1376.3793000000	1410.8831000000	1436.8938000000
1466.9376000000	1510.2582000000	1578.8514000000	1600.9598000000
1656.2681000000	1691.0027000000	1725.1061000000	1833.7879000000
3216.3306000000	3238.1114000000	3250.0879000000	3284.8936000000
3295.7018000000	3301.2328000000	3739.6254000000	3872.9800000000

Figure S1.7. Population dynamics for anionic HBI. Dotted lines are population traces for individual runs and solid line is average over all runs.

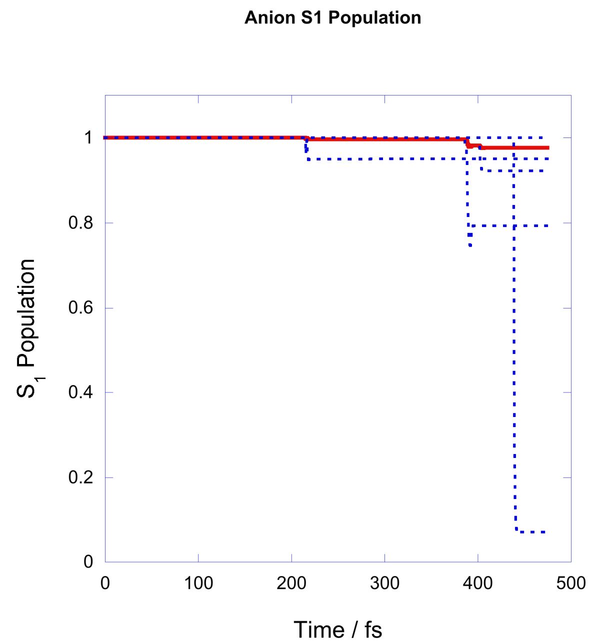

Figure S1.8. Population dynamics for neutral HBI. Dotted lines are population traces for individual runs and solid line is average over all runs.

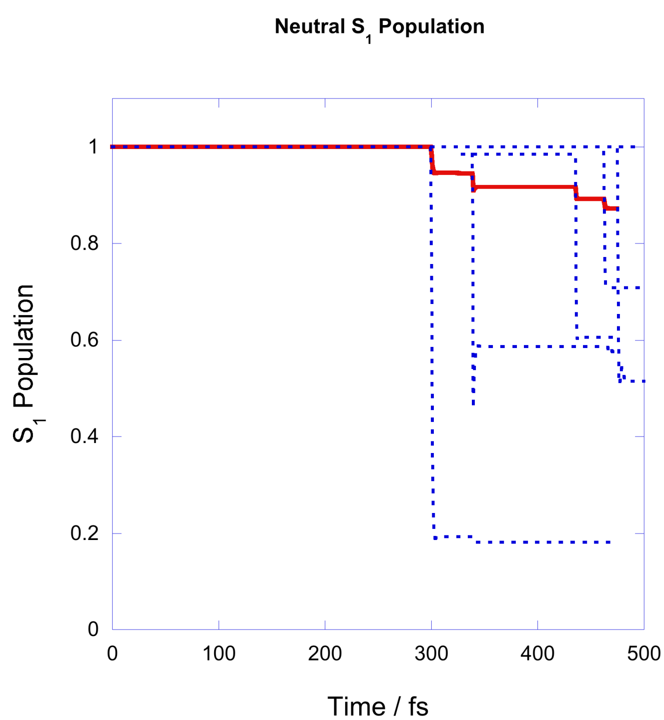

III: Synchronous Transit Plots

Figure 2 displays two synchronous transit plots each for neutral and anionic HBI. One of these is for imidazolinone torsion; one is for phenoxy (phenol) torsion. Each slice begins with the SA2-CAS(2,2)/6-31G S_0 minimum geometry and terminates with a imidazolinone or phenoxy twisted structure. In the anionic case, the twisted structures are minima on the S_1 surface. In the neutral case, the imidazolinone-twisted structure is a true S_1 minimum and the phenoxy-twisted structure was produced by minimization on S_1 under constraint of the dihedrals spanning the bridge-phenol bond. The interpolations were performed in Z-matrix internal coordinates. The symbolic Z-matrices can be found in this section in tables S2.1 (anion) and S2.5 (neutral). Data pertaining to the anchor points can be found in tables S2.2, S2.3 and S2.4 (anion) and S2.5, S2.6 and S2.7 (neutral). Z-matrix variables, SA2-CAS(2,2)/6-31G state energies, and state averaged natural orbitals and occupation numbers are displayed. Multi-reference 2nd order Rayleigh-Schrödinger perturbation theory calculations were performed, which correlated only the highest-lying 32 canonical MCSCF orbitals.

Table S2.1. Symbolic Z-Matrix for anionic HBI used to construct synchronous transit plots in Figure 2. Heavy atom naming scheme is indicated at right.

```
N3I;
H1N3I,   1,   RNH1;
C4I,     1,   RCN2,   2,   ACNH1;
H1C4I,   3,   RCH3,   1,   AHCN2,   2,   DHCNH1;
N5I,     3,   RCN4,   1,   ANCN3,   2,   DNCNH2;
C1I,     5,   RCN5,   3,   ACNC4,   1,   DCNCN3;
C2I,     6,   RCC6,   5,   ACCN5,   3,   DCCNC4;
O1C2I,   7,   RCO7,   1,   AOCN6,   3,   DOCNC5;
C1B,     6,   RCC8,   7,   ACCC7,   8,   DCCCO6;
H1C1B,   9,   RCH9,   6,   AHCC8,   7,   DHCCC7;
C1P,     9,   RCC10,  6,   ACCC9,   5,   DCCCN8;
C2P,     11,  RCC11,  9,   ACCC10,  6,   DCCCC9;
H1C2P,   12,  RCH12,  11,  AHCC11,  9,   DHCCC10;
C3P,     12,  RCC13,  11,  ACCC12,  9,   DCCCC11;
H1C3P,   14,  RCH14,  12,  AHCC13,  11,  DHCCC12;
C4P,     14,  RCC15,  12,  ACCC14,  11,  DCCCC13;
C5P,     16,  RCC16,  14,  ACCC15,  12,  DCCCC14;
H1C5P,   17,  RCH17,  16,  AHCC16,  14,  DHCCC15;
C6P,     17,  RCC18,  16,  ACCC17,  14,  DCCCC16;
H1C6P,   19,  RCH19,  11,  AHCC18,  12,  DHCCC17;
O1C4P,   16,  RCO20,  17,  AOCC19,  19,  DOCCC18;
```

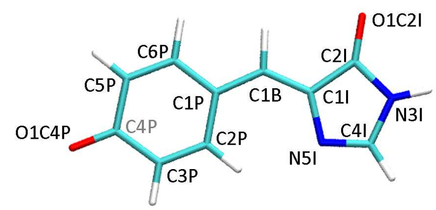

Table S2.2. Z-matrix variables, SA2-CAS(2,2)/6-31G energies and wavefunction (natural orbitals and occupation numbers) at the SA2-CAS(2,2)/6-31G S_0 minimum geometry of anionic HBI.

```
RNH1 = 0.98839073
RCN2 = 1.38724228
ACNH1 = 127.555937
RCH3 = 1.0665974
AHCN2 = 122.2450943
DHCNH1 = 0.00015943
RCN4 = 1.27986638
ANCN3 = 112.1516022
DNCNH2 = -180.0030627
RCN5 = 1.41791742
ACNC4 = 107.1417642
DCNCN3 = 0.00113285
RCC6 = 1.44070452
ACCN5 = 108.6031789
DCCNC4 = 0.00090544
RCO7 = 1.24587208
AOCN6 = 124.2634391
DOCNC5 = -179.9992191
RCC8 = 1.36967715
ACCC7 = 123.9423057
DCCCO6 = -0.00154168
RCH9 = 1.07781284
AHCC8 = 112.6313413
DHCCC7 = 0.00281289
RCC10 = 1.40932609
ACCC9 = 132.2572916
DCCCN8 = -0.00286096
RCC11 = 1.42488788
ACCC10 = 124.5993002
DCCCC9 = 0.01162349
RCH12 = 1.07139774
AHCC11 = 117.963473
DHCCC10 = -0.01241575
RCC13 = 1.35822481
ACCC12 = 121.7314827
DCCCC11 = -180.0096271
RCH14 = 1.07338493
AHCC13 = 121.0263037
DHCCC12 = 179.9963218
RCC15 = 1.44635972
ACCC14 = 122.3095184
DCCCC13 = -0.00248383
RCC16 = 1.44331464
ACCC15 = 115.4046064
DCCCC14 = 0.00723557
RCH17 = 1.07312974
AHCC16 = 117.1167332
DHCCC15 = 179.9924558
RCC18 = 1.35796814
ACCC17 = 121.4315944
DCCCC16 = -0.00480304
RCH19 = 1.07686921
AHCC18 = 117.9797837
DHCCC17 = -179.9958133
RCO20 = 1.25800184
AOCC19 = 122.3834332
DOCCC18 = -180.0027046
```

State Energies: $E(S_0)$= -641.134677143971a.u., $E(S_1)$= -640.981785421320a.u.

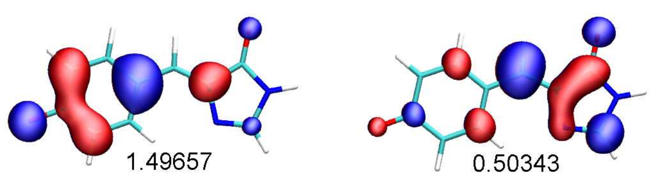

Table S2.3. SA2-CAS(2,2)/6-31G wavefunction (natural orbitals and occupation numbers) at the SA2-CAS(2,2)/6-31G imidazolinone-twisted S_1 minimum geometry of anionic HBI.

RNH1 = 0.98898101	ACCC7 = 127.1034211	DHCCC12 = 179.915215
RCN2 = 1.36972246	DCCCO6 = -1.53702504	RCC15 = 1.43664735
ACNH1 = 127.527152	RCH9 = 1.07606855	ACCC14 = 122.490857
RCH3 = 1.06593287	AHCC8 = 116.4758056	DCCCC13 = 0.0293163
AHCN2 = 122.6267664	DHCCC7 = 89.23177397	RCC16 = 1.43825092
DHCNH1 = -0.19245716	RCC10 = 1.41377277	ACCC15 = 114.5621832
RCN4 = 1.29988569	ACCC9 = 124.8932657	DCCCC14 = -0.07494423
ANCN3 = 112.6614255	DCCCN8 = 89.13391817	RCH17 = 1.07419354
DNCNH2 = -180.2508357	RCC11 = 1.42034181	AHCC16 = 116.9249932
RCN5 = 1.38888806	ACCC10 = 123.9568131	DHCCC15 = 180.0404366
ACNC4 = 107.8602641	DCCCC9 = 0	RCC18 = 1.3643568
DCNCN3 = -0.38929474	RCH12 = 1.07572478	ACCC17 = 122.281233
RCC6 = 1.46776178	AHCC11 = 118.6981392	DCCCC16 = 0.01824928
ACCN5 = 107.7756662	DHCCC10 = -0.35453096	RCH19 = 1.07752641
DCCNC4 = 0.80716738	RCC13 = 1.3666297	AHCC18 = 117.9978866
RCO7 = 1.22686531	ACCC12 = 122.5080952	DHCCC17 = -180.0990483
AOCN6 = 124.5667835	DCCCC11 = -179.9317025	RCO20 = 1.27048623
DOCNC5 = -178.2331084	RCH14 = 1.07413308	AOCC19 = 122.6399864
RCC8 = 1.44643914	AHCC13 = 120.6359164	DOCCC18 = -179.87464

State Energies: $E(S_0)$= -641.057725851047a.u., $E(S_1)$= -641.028987216418a.u.

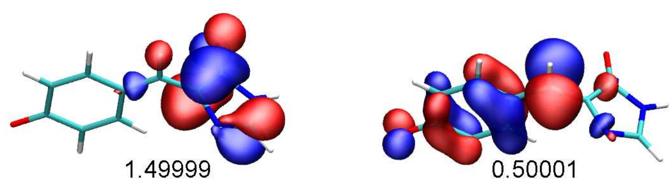

Table S2.4. SA2-CAS(2,2)/6-31G wavefunction (natural orbitals and occupation numbers) at the SA2-CAS(2,2)/6-31G phenoxy-twisted S_1 minimum geometry of anionic HBI.

RNH1 = 0.98804731	ACCC7 = 126.3143928	DHCCC12 = 180.0378176
RCN2 = 1.38144953	DCCCO6 = -0.01406547	RCC15 = 1.45292565
ACNH1 = 127.7510349	RCH9 = 1.074493	ACCC14 = 121.3036302
RCH3 = 1.06619312	AHCC8 = 118.4580337	DCCCC13 = 0.25477269
AHCN2 = 123.0248017	DHCCC7 = -0.00217385	RCC16 = 1.45290763
DHCNH1 = -0.0018087	RCC10 = 1.46689321	ACCC15 = 116.1733169
RCN4 = 1.29279084	ACCC9 = 123.0857428	DCCCC14 = 0.65176314
ANCN3 = 111.0975668	DCCCN8 = -0.0100309	RCH17 = 1.07242624
DNCNH2 = -180.0030577	RCC11 = 1.43139666	AHCC16 = 116.7601303
RCN5 = 1.40381921	ACCC10 = 121.6120072	DHCCC15 = 179.1490988
ACNC4 = 107.3762956	DCCCC9 = 90.74036231	RCC18 = 1.35288832
DCNCN3 = 0.00287636	RCH12 = 1.07207965	ACCC17 = 121.3012906
RCC6 = 1.42159756	AHCC11 = 117.1923516	DCCCC16 = -0.64445161
ACCN5 = 109.3176481	DHCCC10 = -2.75442664	RCH19 = 1.07208034
DCCNC4 = -0.0029787	RCC13 = 1.35288801	AHCC18 = 117.1902519
RCO7 = 1.26372224	ACCC12 = 122.2219344	DHCCC17 = -178.6555591
AOCN6 = 123.822966	DCCCC11 = -182.550239	RCO20 = 1.24633245
DOCNC5 = -179.9955951	RCH14 = 1.07242572	AOCC19 = 121.9165653
RCC8 = 1.40227331	AHCC13 = 121.9392931	DOCCC18 = -180.7506295

State Energies: $E(S_0)$= -641.066602608222a.u., $E(S_1)$=-641.028986128020a.u.

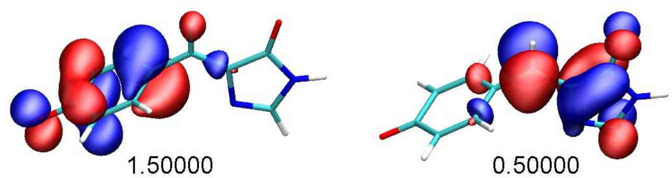

Table S2.5. Symbolic Z-Matrix for neutral HBI used to generate the synchronous transit plots in Figure 2. Heavy atom naming system is indicated at right.

```
N3I;
H1N3I,   1,   RNH1;
C4I,     1,   RCN2,   2,   ACNH1;
H1C4I,   3,   RCH3,   1,   AHCN2,   2,   DHCNH1;
N5I,     3,   RCN4,   1,   ANCN3,   2,   DNCNH2;
C1I,     5,   RCN5,   3,   ACNC4,   1,   DCNCN3;
C2I,     6,   RCC6,   5,   ACCN5,   3,   DCCNC4;
O1C2I,   7,   RCO7,   1,   AOCN6,   3,   DOCNC5;
C1B,     6,   RCC8,   7,   ACCC7,   8,   DCCCO6;
H1C1B,   9,   RCH9,   6,   AHCC8,   7,   DHCCC7;
C1P,     9,   RCC10,  6,   ACCC9,   5,   DCCCN8;
C2P,     11,  RCC11,  9,   ACCC10,  6,   DCCCC9;
H1C2P,   12,  RCH12,  11,  AHCC11,  9,   DHCCC10;
C3P,     12,  RCC13,  11,  ACCC12,  9,   DCCCC11;
H1C3P,   14,  RCH14,  12,  AHCC13,  11,  DHCCC12;
C4P,     14,  RCC15,  12,  ACCC14,  11,  DCCCC13;
C5P,     16,  RCC16,  14,  ACCC15,  12,  DCCCC14;
H1C5P,   17,  RCH17,  16,  AHCC16,  14,  DHCCC15;
C6P,     17,  RCC18,  16,  ACCC17,  14,  DCCCC16;
H1C6P,   19,  RCH19,  11,  AHCC18,  12,  DHCCC17;
O1C4P,   16,  RCO20,  17,  AOCC19,  19,  DOCCC18;
H1O1C4P, 21,  ROH21,  16,  AHOC20,  17,  DHOCC19;
```

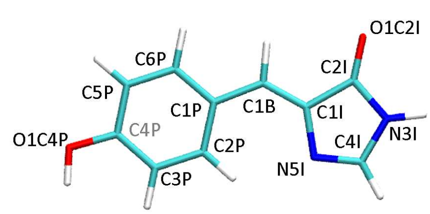

Table S2.6. Z-Matrix variables, SA2-CAS(2,2)/6-31G state-specific energies, state-averaged natural orbitals and occupation numbers at the SA2-CAS(2,2)/6-31G S_0 minimum geometry of neutral HBI.

RNH1 = 0.99024568	ACNH1 = 127.0264361	AHCN2 = 122.0994418
RCN2 = 1.38309897	RCH3 = 1.06567993	DHCNH1 = 0.00005509

```
RCN4 = 1.2837399
ANCN3 = 112.842033
DNCNH2 = -179.9994849
RCN5 = 1.40732981
ACNC4 = 106.8400836
DCNCN3 = -0.00044335
RCC6 = 1.46206112
ACCN5 = 108.5538833
DCCNC4 = 0.00023353
RCO7 = 1.22524578
AOCN6 = 126.3214916
DOCNC5 = -179.9973339
RCC8 = 1.36142108
ACCC7 = 123.4447473
DCCCO6 = -0.00760777
RCH9 = 1.07660804
AHCC8 = 113.6979676
DHCCC7 = -0.00484638
RCC10 = 1.43634501
ACCC9 = 130.7417748
DCCCN8 = -0.00895221
RCC11 = 1.39766411
ACCC10 = 123.8267263
DCCCC9 = 0.00201811
RCH12 = 1.06979664
AHCC11 = 119.5094351
DHCCC10 = 0.00922103
RCC13 = 1.38432545
ACCC12 = 120.6213968
DCCCC11 = -180.0046082
RCH14 = 1.07418046
AHCC13 = 119.7879747
DHCCC12 = 180.0038069
RCC15 = 1.3859778
ACCC14 = 119.9990346
DCCCC13 = 0.00875214
RCC16 = 1.38575624
ACCC15 = 120.5673127
DCCCC14 = -0.00797625
RCH17 = 1.07049408
AHCC16 = 119.0710828
DHCCC15 = 180.0051979
RCC18 = 1.37850434
ACCC17 = 119.1814246
DCCCC16 = 0.00590629
RCH19 = 1.07412736
AHCC18 = 119.3980212
DHCCC17 = -180.0044008
RCO20 = 1.37392175
AOCC19 = 116.9577667
DOCCC18 = -179.9918007
ROH21 = 0.94969921
AHOC20 = 114.8967055
DHOCC19 = 179.982536
```

State Energies: $E(S_0)$= -641.689768624901a.u., $E(S_1)$= -641.504617086528a.u.

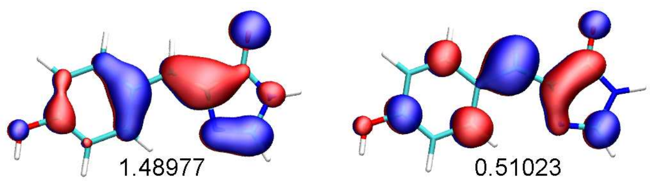

Table S2.7. Z-Matrix variables, SA2-CAS(2,2)/6-31G state-specific energies, natural orbitals, and occupation numbers at the SA2-CAS(2,2)/6-31G imidazolinone-twisted S_1 minimum geometry (I-S_1) of neutral HBI.

RNH1 = 0.98941966	DCCCO6 = 4.99940588	ACCC14 = 119.1036035
RCN2 = 1.37878661	RCH9 = 1.08485622	DCCCC13 = -0.1557123
ACNH1 = 127.4511892	AHCC8 = 119.339896	RCC16 = 1.40463975
RCH3 = 1.0647052	DHCCC7 = 86.23092499	ACCC15 = 121.8746539
AHCN2 = 123.3527032	RCC10 = 1.38554289	DCCCC14 = 0.11233919
DHCNH1 = 0.80672723	ACCC9 = 125.737175	RCH17 = 1.06928865
RCN4 = 1.29242572	DCCCN8 = 92.29029272	AHCC16 = 118.4936529
ANCN3 = 111.1783765	RCC11 = 1.42024789	DHCCC15 = 180.150447
DNCNH2 = -179.2886177	ACCC10 = 120.633589	RCC18 = 1.36244462
RCN5 = 1.40183974	DCCCC9 = 0	ACCC17 = 118.8188881
ACNC4 = 105.7658972	RCH12 = 1.07015723	DCCCC16 = -0.12323916
DCNCN3 = -0.2555019	AHCC11 = 117.9025773	RCH19 = 1.07294477
RCC6 = 1.40107804	DHCCC10 = -0.04238455	AHCC18 = 118.9496354
ACCN5 = 111.5234395	RCC13 = 1.3698882	DHCCC17 = -180.3256259
DCCNC4 = 0.70226806	ACCC12 = 120.6584656	RCO20 = 1.34337353
RCO7 = 1.26157638	DCCCC11 = -180.2359945	AOCC19 = 116.0583428
AOCN6 = 125.3598727	RCH14 = 1.07222171	DOCCC18 = -180.1210721
DOCNC5 = -180.1556941	AHCC13 = 120.8028564	ROH21 = 0.95151869
RCC8 = 1.43891505	DHCCC12 = 180.1863061	AHOC20 = 116.7636177
ACCC7 = 125.9177922	RCC15 = 1.39902907	DHOCC19 = 180.640953

State Energies: E(S_0)= -641.591432700723a.u., E(S_1)= -641.567861072717a.u.

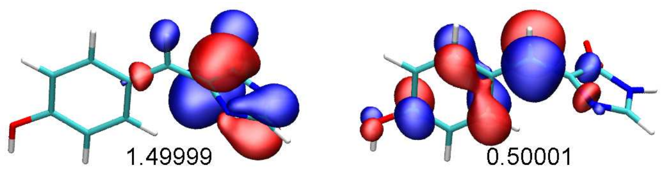

Table S2.8. Z-Matrix variables, SA2-CAS(2,2)/6-31G wavefunction (natural orbitals and occupation numbers) at the SA2-CAS(2,2)/6-31G phenoxy-twisted constrained S_1-minimized geometry of neutral HBI.

```
RNH1 = 0.9890551
RCN2 = 1.37672306
ACNH1 = 127.3130858
RCH3 = 1.06543325
AHCN2 = 122.971844
DHCNH1 = -0.29330991
RCN4 = 1.29451412
ANCN3 = 111.3272858
DNCNH2 = -180.3139217
RCN5 = 1.40416116
ACNC4 = 106.9817349
DCNCN3 = 0.09988309
RCC6 = 1.42591649
ACCN5 = 109.6378464
DCCNC4 = -0.09665712
RCO7 = 1.2503832
AOCN6 = 125.0408595
DOCNC5 = -180.0819668
RCC8 = 1.39570015
ACCC7 = 128.091763
DCCCO6 = -0.21265435
RCH9 = 1.07257927
AHCC8 = 122.2621973
DHCCC7 = 0.95465654
RCC10 = 1.45230819
ACCC9 = 117.3463214
DCCCN8 = 0
RCC11 = 1.44629463
ACCC10 = 121.2810303
DCCCC9 = 90
RCH12 = 1.06979965
AHCC11 = 116.9967609
DHCCC10 = 0.43704345
RCC13 = 1.35931323
ACCC12 = 121.7935141
DCCCC11 = -178.9149306
RCH14 = 1.07264526
AHCC13 = 121.2816187
DHCCC12 = 179.7369214
RCC15 = 1.41119446
ACCC14 = 118.9072932
DCCCC13 = 0.57171643
RCC16 = 1.4152541
ACCC15 = 121.6922384
DCCCC14 = -0.29675164
RCH17 = 1.06974569
AHCC16 = 118.0111284
DHCCC15 = 179.4547029
RCC18 = 1.35528429
ACCC17 = 119.1370115
DCCCC16 = 0.28239262
RCH19 = 1.06950943
AHCC18 = 117.0597671
DHCCC17 = -178.5201507
RCO20 = 1.33175469
AOCC19 = 116.197593
DOCCC18 = -179.7250438
ROH21 = 0.95245584
AHOC20 = 117.5897216
DHOCC19 = 178.7
```

State Energies: $E(S_0)$= -641.639876961157a.u., $E(S_1)$= -641.506033089692a.u.

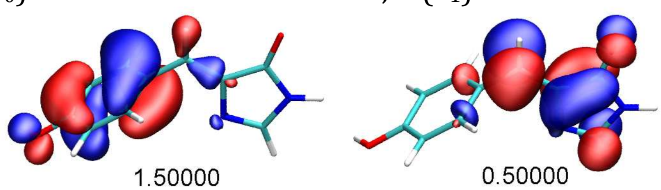

IV: Propriety of the Electronic Structure Ansatz

Here, we present data, which we obtained in order to verify that the SA2-CAS(2,2)/6-31g electronic structure ansatz, used in the on-the-fly dynamics calculations, is reasonable. We do this by examining changes in the predicted geometries and energies of important critical points on the S_0 and S_1 surfaces. For the anion, three geometries are described: the Frank-Condon geometry (S_0-minimum), and two S_1 minima, which are twisted about the phenoxy-methine (P-S_1) or imidazolinone-methine (I-S_1) bond. An analogous set was examined for the neutral form, but in this case there is no stable phenoxy-twisted form on the S_1 state. Instead of P-S_1 as for the anion, we use a structure obtained by S_1-optimization under dihedral constraint on the phenoxy-methine bond. Each geometry was optimized using three model spaces: SA2-CAS(2,2)/6-31g, SA2-CAS(2,2)/6-31G* and SA2-CAS(4,3)/6-31g*. These data examine, therefore, the consequences both of enlarging the one-body basis or the many-body basis. Table S3.1 lists bond lengths (Å) for the optimized structures of the anion. Table S3.2 displays heavy-atom bond lengths (Å) for the neutral form, and Tables S3.1 and S3.2 list energetic and dipole data for the anion and neutral, respectively, evaluated with SA2-CAS(2,2)/6-31g, SA2-CAS(2,2)/6-31g* and SA2-CAS(4,3)/6-31g* with and without correction with MR-RSPT2. Only the highest 32 orbitals were correlated in the MR-RSPT2.

Comparisons can also be made with CASSCF and MRPT2 calculations in the existing literature. For example, Vendrell et al. report a vertical excitation energy of 3.69 eV for neutral HBI using single-state CAS(6,6)*MR-RSPT2 calculations and a 6-31g basis set.[13] Martin et al.[14] and Sinicropi et al.[15] report a vertical excitation energy of 2.67 eV for anionic HBI using a SA2-CAS(12,11)*MR-RSPT2 ansatz and a 6-31g* basis set. The same authors report a difference dipole norm of 1.0 D for the S_0-S_1 transition in anionic HBI. All of these results are in close agreement with our own, confirming that our electronic structure methodology is appropriate for the problem.

Table S3.1. Heavy-atom bond lengths (Å) for S_0 and S_1 critical points for anionic HBI, optimized using three model spaces: SA2-CAS(2,2)/6-31g, SA2-CAS(2,2)/6-31G* and SA2-CAS(4,3)/6-31G*. As shown, the effect of enlarging the one-electron or many-electron bases is small. The bond alternation is maintained, indicating that each ansatz targets the same states.

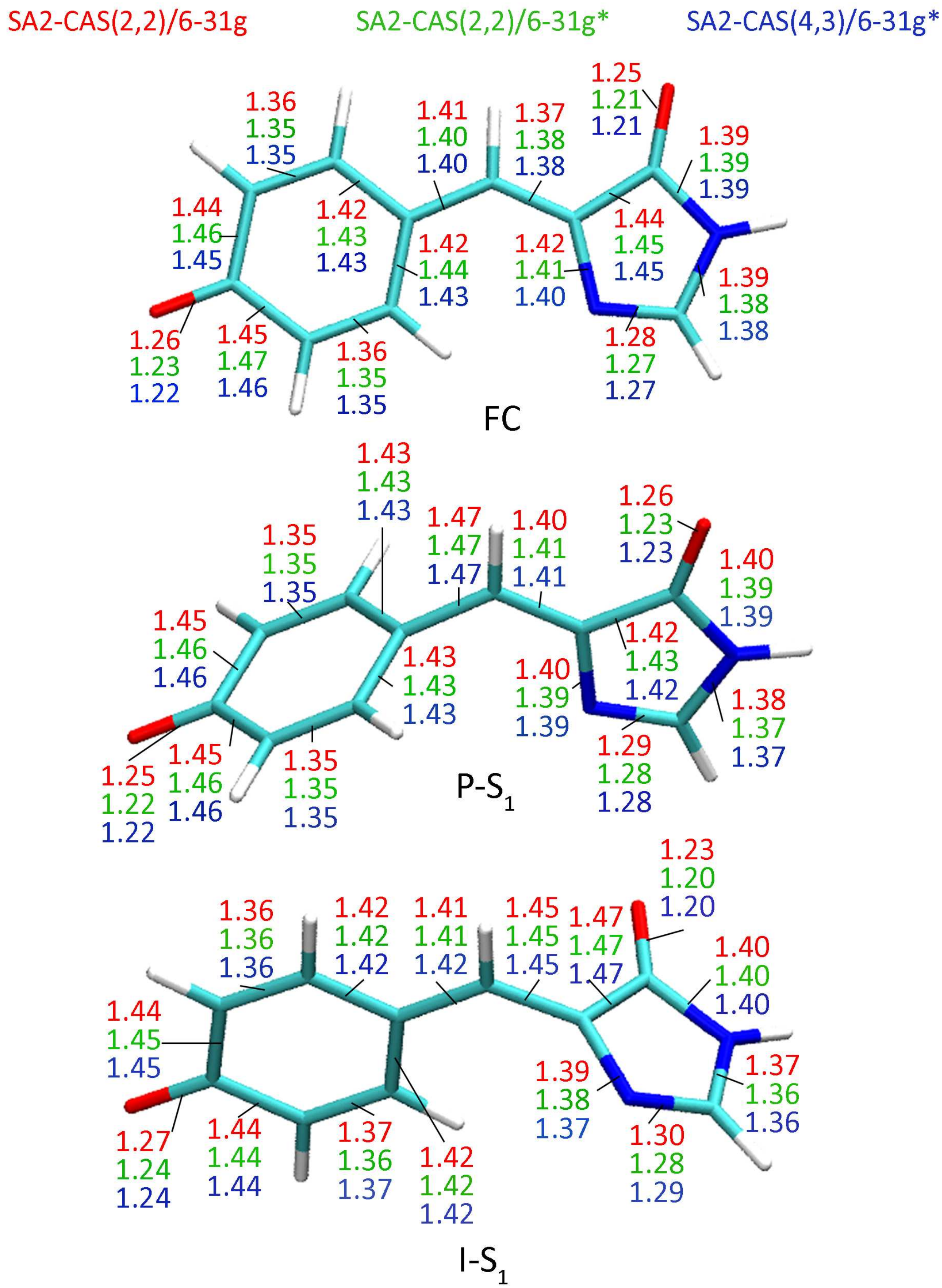

Figure S3.2. Heavy-atom bond lengths (Å) for S_0 and S_1 critical points for anionic HBI, optimized using three model spaces: SA2-CAS(2,2)/6-31g, SA2-CAS(2,2)/6-31G* and SA2-CAS(4,3)/6-31G*. Geometries are the Frank Condon geometry (FC, top), imidazolinone-twisted S_1 minimum (I-S_1, bottom right), and a structure minimized on S_1 under constraint of a twisted phenoxy-methine bond (P-$S_{1C,}$ bottom left). This titration state has no stable S_1 structure with a twisted phenoxy-methine bond. As shown, the effect of enlarging the one-electron or many-electron bases is small. The bond alternation is maintained, indicating that each ansatz targets the same states.

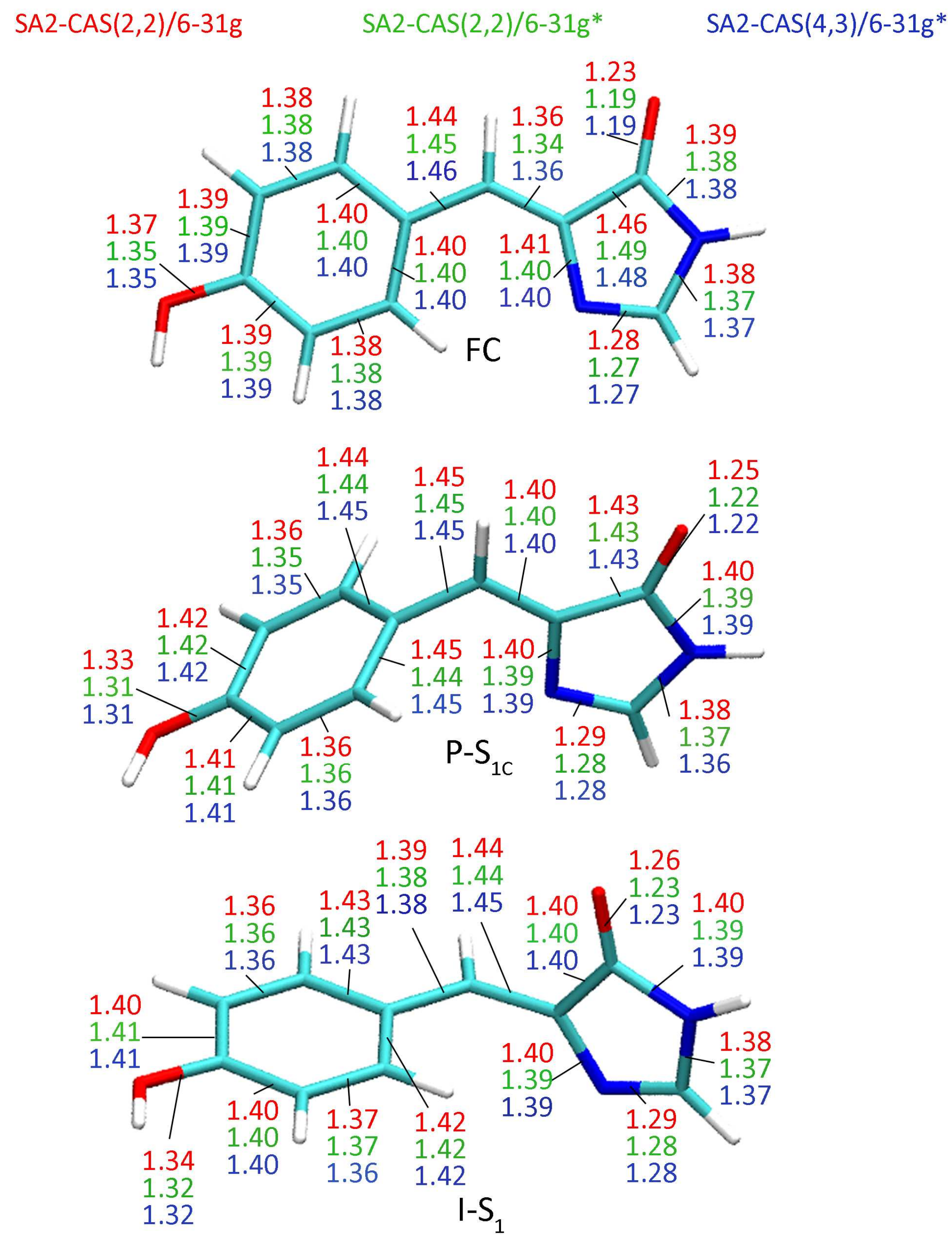

Table S3.1. State-specific energies (kcal/mol, relative to S_0 energy at FC), S_0-S_1 excitation energies (eV), state-specific dipole norms, S_1-S_0 difference dipole norms and transition dipole norms (D) for the FC, I-S_1 and P-S_1 geometries of anionic HBI. Data were taken at geometries optimized with the CASSCF and basis specified. Italic quantities are calculated from the SA-CASSCF, while bold quantities include the correction applied by second order multi-reference Rayleigh-Schrödinger perturbation theory (MR-RSPT2). MR-RSPT2 calculations correlated the highest 32 occupied orbitals of the reference space.

Geo.	CAS	Bas.	$E(S_0)$	$E(S_1)$	$\Delta E(S_1\text{-}S_0)$	$\vert\mu(S_0)\vert$	$\vert\mu(S_1)\vert$	$\vert\Delta\mu\vert$	$\vert\langle S_0\vert\mu\vert S_1\rangle\vert$
FC	(2,2)	6-31g	*0.0* **0.0**	*95.9* **58.9**	*4.16* **2.56**	*7.4* **7.5**	*8.0* **7.9**	***0.6*** **0.5**	*9.6* **9.5**
FC	(2,2)	6-31g*	*0.0* **0.0**	*98.1* **60.3**	*4.25* **2.61**	*7.5* **7.6**	*7.5* **7.5**	*0.1* **0.2**	*9.3* **9.2**
FC	(4,3)	6-31g*	*0.0* **0.0**	*94.7* **62.5**	*4.11* **2.71**	*8.1* **7.9**	*6.8* **6.7**	*1.3* **1.2**	*10.0* **9.6**
I-S_1	(2,2)	6-31g	*48.3* **31.8**	*66.3* **49.4**	*0.78* **0.77**	*3.3* **3.0**	*15.0* **14.5**	*13.7* **13.1**	*0.1* **0.1**
I-S_1	(2,2)	6-31g*	*49.7* **34.7**	*64.0* **49.2**	*0.62* **0.63**	*2.5* **2.4**	*14.1* **13.7**	*13.4* **12.8**	*0.2* **0.2**
I-S_1	(4,3)	6-31g*	*44.5* **34.8**	*69.5* **50.3**	*1.08* **0.67**	*2.3* **2.1**	*15.0* **14.5**	*15.2* **14.4**	*0.2* **0.2**
P-S_1	(2,2)	6-31g	*42.7* **28.0**	*66.3* **48.4**	*1.02* **0.88**	*14.3* **13.6**	*3.3* **2.7**	*16.2* **15.0**	*0.1* **0.0**
P-S_1	(2,2)	6-31g*	*40.6* **27.3**	*68.1* **52.3**	*1.19* **1.08**	*13.7* **13.2**	*3.0* **2.6**	*15.4* **14.4**	*0.1* **0.1**
P-S_1	(4,3)	6-31g*	*35.0* **27.6**	*73.7* **53.1**	*1.68* **1.11**	*14.5* **13.8**	*3.2* **2.7**	*16.6* **15.5**	*0.1* **0.1**

Table S3.2. State-specific energies (kcal/mol, relative to S_0 energy at FC), S_0-S_1 excitation energies (eV), state-specific dipole norms, S_1-S_0 difference dipole norms and transition dipole norms (D) for the FC, I-S_1 and P-S_1 geometries of neutral HBI. Data were taken at geometries optimized with the CASSCF and basis specified. Italic quantities are calculated from the SA-CASSCF, while bold quantities include the correction applied by second order multi-reference Rayleigh-Schrödinger perturbation theory (MR-RSPT2). MR-RSPT2 calculations correlated the highest 32 occupied orbitals of the reference space.

Geo.	CAS	Bas.	$E(S_0)$	$E(S_1)$	$\Delta E(S_1\text{-}S_0)$	$\lvert\mu(S_0)\rvert$	$\lvert\mu(S_1)\rvert$	$\lvert\Delta\mu(S_1\text{-}S_0)\rvert$	$\lvert\langle S_0\lvert\mu\rvert S_1\rangle\rvert$
FC	(2,2)	6-31g	*0.0* **0.0**	*116.2* **86.2**	*5.03* **3.74**	*3.9* **4.0**	*5.2* **5.1**	*3.0* **3.0**	*7.0* **7.2**
FC	(2,2)	6-31g*	*0.0* **0.0**	*119.2* **87.8**	*5.17* **3.79**	*3.8* **3.8**	*5.1* **5.1**	*3.3* **3.5**	*7.3* **7.3**
FC	(4,3)	6-31g*	*0.0* **0.0**	*121.7* **89.9**	*5.27* **3.90**	*3.9* **3.9**	*7.3* **6.7**	*6.8* **6.0**	*7.6* **7.3**
I-S_1	(2,2)	6-31g	*61.7* **39.7**	*76.5* **67.2**	*0.64* **1.19**	*4.9* **4.5**	*9.2* **9.2**	*11.8* **11.4**	*0.1* **0.0**
I-S_1	(2,2)	6-31g*	*62.0* **41.2**	*78.9* **67.6**	*0.73* **1.14**	*4.5* **4.1**	*9.5* **9.5**	*11.7* **11.3**	*0.1* **0.0**
I-S_1	(4,3)	6-31g*	*66.1* **47.4**	*77.8* **70.7**	*0.51* **1.01**	*4.7* **4.2**	*10.7* **10.4**	*13.4* **12.6**	*0.1* **0.1**
P-S_{1C}	(2,2)	6-31g	*31.2* **8.3**	*115.3* **99.7**	*3.65* **3.97**	*3.0* **3.1**	*14.7* **14.1**	*14.7* **13.5**	*0.2* **0.2**
P-S_{1C}	(2,2)	6-31g*	*30.1* **8.8**	*116.2* **99.7**	*3.74* **3.94**	*3.0* **3.1**	*14.4* **13.8**	*14.7* **13.4**	*0.2* **0.2**
P-S_{1C}	(4,3)	6-31g*	*22.4* **11.2**	*122.3* **103.3**	*4.33* **3.99**	*3.1* **3.2**	*14.2* **13.7**	*14.4* **13.4**	*0.1* **0.1**

V: Two-Dimensional Interpolation Surfaces for Neutral and Anionic HBI with different active spaces

This section contains 2-dimensional linear interpolation (synchronous transit) surfaces for neutral and anionic HBI calculated using SA-CASSCF and MR-RSPT2 theoretical models with 2-electron, 2-orbital and 4-electron, 3-orbital active spaces. They show that the features of the potential surface are well-converged at the level of the SA2-CAS(2,2) ansatz which was used for the AIMS dynamical simulations.

The two-dimensional interpolations were generated from three anchor geometries for each ionic form. For the anion, the anchors were the Frank-Condon (FC) geometry (S_0 minimum), and excited state minima twisted about the imidazolinone (I-S_1) and phenoxy (P-S_1) bonds of the chromophore. For the neutral form, the Frank-Condon geometry and an imidazolinone twisted minimum were also used. There is no phenoxy-twisted stable minimum for neutral HBI, so the third anchor was a S_1 relaxed geometry that was constrained to be twisted about the phenoxy bond and planar about the imidazolinone bond (P-S_{1C}). The geometries were optimized on the SA2-CAS(2,2) surfaces.

The similarity between the results obtained for 2-electron, 2-orbital and 4-electron, 3-orbital active spaces shows that the dynamics should be robust. If the two-electron, two-orbital active space was not sufficient, then we would expect to see an initial large change in the behavior upon enlargement of the active space, followed by decreasing effects with further increases in the active space rank. The lack of change seen here shows that the rank is sufficient.

The linear interpolation slices in Fig. 2 of the main text are diagonal slices through the 2-D interpolations in Fig. S4.1 (anion) and Fig. S4.2 (neutral) at the same level of theory.

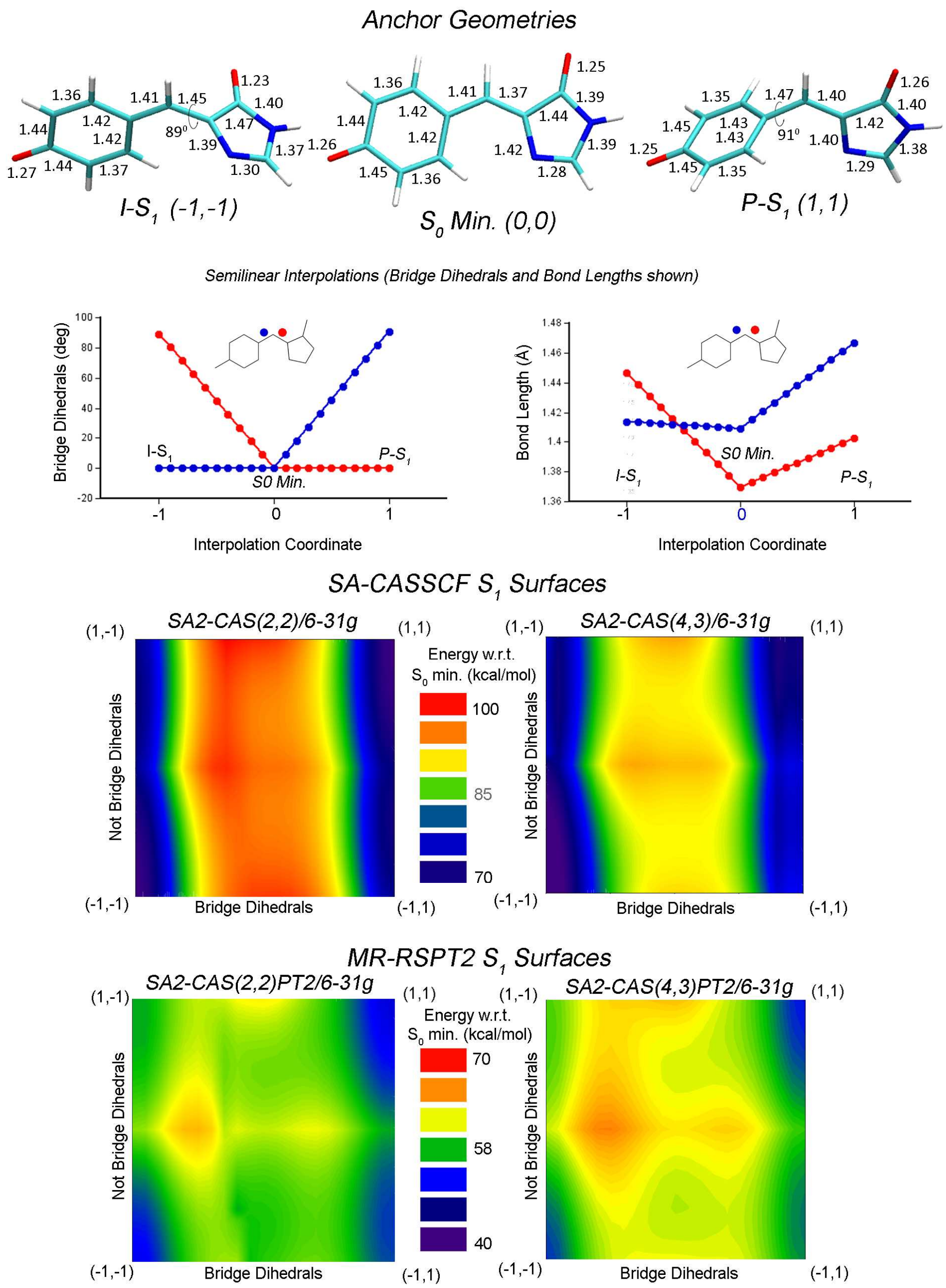

Figure S4.1. *Top:* SA2-CAS(2,2)/6-31g optimized imidazolinone-twisted S_1 minimum (I-S_1, left), S_0 minimum (S_0 Min, center) and phenoxy-twisted S_1 minimum (P-S_1, right). *Middle*: Bilinear interpolation pathways in symbolic Z-matrix variables connecting I-S_1, S_0 Min and P-S_1 min (bridge dihedrals and bond lengths shown). *Bottom*: 2-dimensional synchronous semilinear transit surfaces calculated with different methodologies. Z-matrix variables were partitioned into two sets, one containing bridge dihedrals and one containing everything else. The horizontal coordinate parametrizes synchronous parabolic transit along the paths of the bridge dihedrals; the vertical coordinate parametrizes synchronous semilinear transit along the paths of the remaining Z-matrix variables (the latter set includes the bridge bonds shown above).

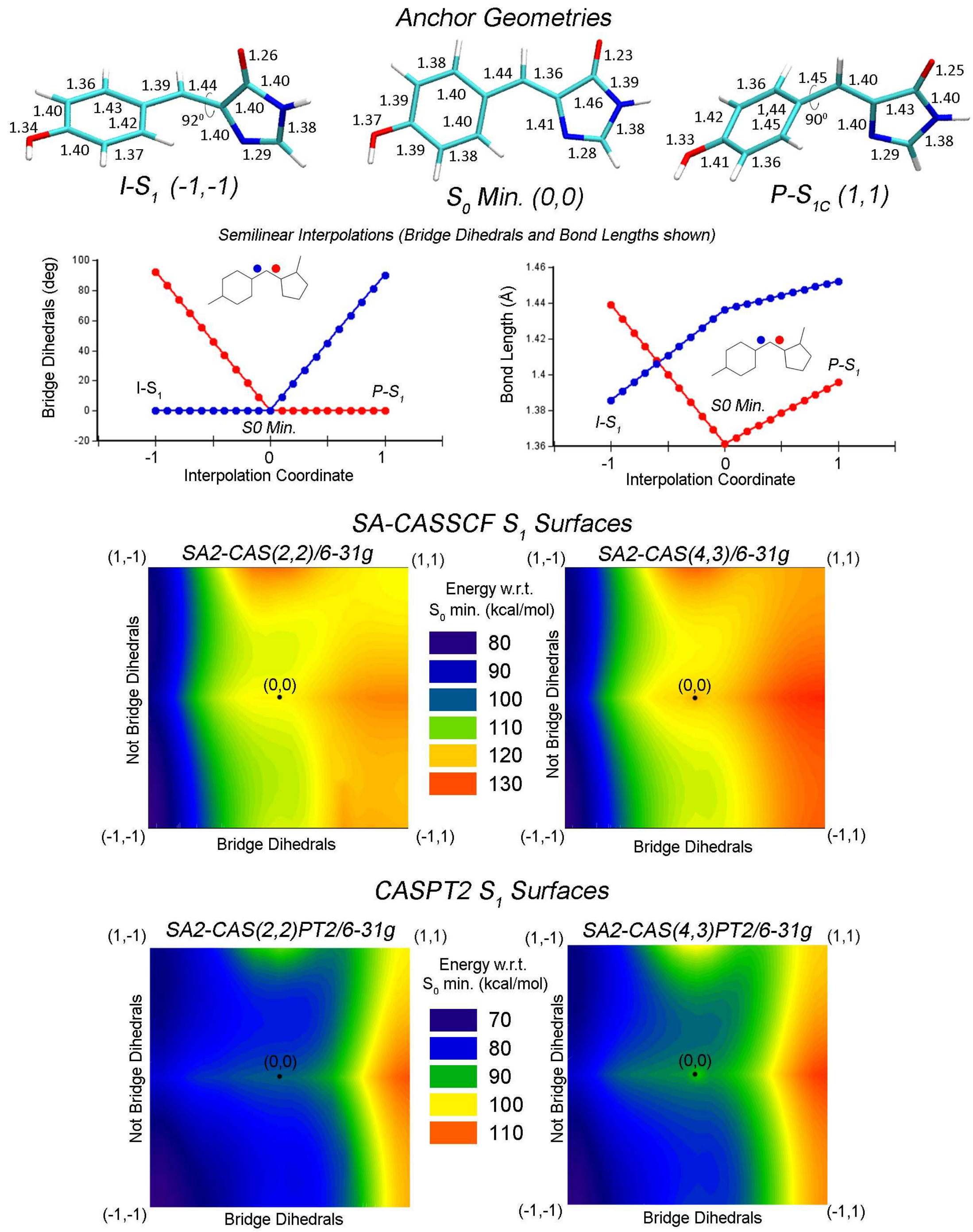

Figure S4.2. *Top:* SA2-CAS(2,2)/6-31g optimized imidazolinone-twisted S_1 minimum (I-S_1, left), S_0 minimum (S_0 Min, center) and phenoxy-constrained S_1 relaxed geometry (P-S_{1C}, right) of neutral HBI. *Middle*: Bilinear interpolation pathways in symbolic Z-matrix variables connecting I-S_1, S_0 Min and P-S_1 min (bridge dihedrals and bond lengths shown). *Bottom*: 2-dimensional synchronous semilinear transit surfaces calculated with different methodologies. Z-matrix variables were partitioned into two sets, one containing bridge dihedrals and one containing everything else. The horizontal coordinate parametrizes synchronous parabolic transit along the paths of the bridge dihedrals; the vertical coordinate parametrizes synchronous semilinear transit along the paths of the remaining Z-matrix variables (the latter set includes the bridge bonds shown above).

IV: References

(1)Levine, B. G.; Coe, J. D.; Virshup, A. M.; Martínez, T. J., *Chem. Phys.* **2008**, *347*, 3-16.
(2) MOLPRO, version 2008.1, a package of ab initio programs, H.-J. Werner, P. J. Knowles, R. Lindh, F. R. Manby, M. Schütz, P. Celani, T. Korona, A. Mitrushenkov, G. Rauhut, T. B. Adler, R. D. Amos, A. Bernhardsson, A. Berning, D. L. Cooper, M. J. O. Deegan, A. J. Dobbyn, F. Eckert, E. Goll, C. Hampel, G. Hetzer, T. Hrenar, G. Knizia, C. Köppl, Y. Liu, A. W. Lloyd, R. A. Mata, A. J. May, S. J. McNicholas, W. Meyer, M. E. Mura, A. Nicklass, P. Palmieri, K. Pflüger, R. Pitzer, M. Reiher, U. Schumann, H. Stoll, A. J. Stone, R. Tarroni, T. Thorsteinsson, M. Wang, and A. Wolf, , see http://www.molpro.net.
(3)Stalring, J.; Bernhardsson, A.; Lindh, R., *Mol. Phys.* **2001**, *99*, 103-114.
(4)Roos, B. O. In *Ab Initio Methods in Quantum Chemistry II*; Lawley, K. P., Ed.; John Wiley and Sons: New York, 1987, p 399.
(5)Frisch, M. J.; Pople, J. A.; Binkley, J. S., *J. Chem. Phys.* **1984**, *80*, 3265-3269.
(6)Hehre, W. J.; Ditchfield, R.; Pople, J. A., *J. Chem. Phys.* **1972**, *56*, 2257-2261.
(7)Krishnan, R.; Binkley, J. S.; Pople, J. A., *J. Chem. Phys.* **1980**, *72*, 650-654.
(8)Møller, C.; Plesset, M. S., *Phys. Rev.* **1934**, *46*, 618.
(9)Celani, P.; Werner, H.-J., *J. Chem. Phys.* **2000**, *112*, 5546-5557.
(10)Tsien, R. Y., *Ann. Rev. Biochem.* **1998**, *67*, 509-544.
(11)Nielsen, S. B.; Lapierre, A.; Andersen, J. U.; Pedersen, U. V.; Tomita, S.; Anderson, L. H., *Phys. Rev. Lett.* **2001**, *87*, 228102/1-4.
(12)Lammich, L.; Petersen, M. A.; Nielsen, M. B.; Andersen, L. H., *Biophys. J.* **2007**, *92*, 201-207.
(13)Vendrell, O.; Gelabert, R.; Moreno, M.; Lluch, J. M., *Chem. Phys. Lett.* **2004**, *396*, 202-207.
(14)Martin, M. E.; Negri, F.; Olivucci, M., *J. Am. Chem. Soc.* **2004**, *126*, 5452-5464.
(15)Sinicropi, A.; Andruniow, T.; Ferré, N.; Basosi, R.; Olivucci, M., *J. Am. Chem. Soc.* **2005**, *127*, 11534-11535.